Anode Materials

DOI: 10.1002/anie.201209689

High Capacity and Rate Capability of Amorphous Phosphorus for Sodium Ion Batteries**

*Jiangfeng Qian, Xianyong Wu, Yuliang Cao, Xinping Ai, and Hanxi Yang**

Sodium ion batteries have recently received renewed interest as a low cost alternative to lithium ion batteries for large-scale electric storage applications, because of the high availability of sodium sources, and the similar chemistry of sodium and lithium.[1–4] However, because Na ions have a much larger radius (1.02 Å) than Li ions (0.76 Å) and preferably coordinate in octahedral or prismatic sites, it is difficult to find crystalline host materials that have adequate electrochemical capacity and cyclability for a sodium ion insertion reaction. In the past decade, a large variety of host materials, such as layered oxides,[5,6] polyanion fluorophosphates,[7–9] hexacyanoferrate,[10–12] and organic polymers,[13,14] has been demonstrated as sodium ion insertion cathodes, with certain redox capacity and cycleability. In contrast, anodic host materials for sodium ion storage are less successful, with very limited choices available.

In earlier development of sodium ion batteries, the anodic materials used were mostly hard carbon materials.[15,16] These anodes demonstrated modest capacity (approximately 200 $mA\,h\,g^{-1}$), but their cycling stability and initial current efficiency are much inferior to those in lithium ion batteries. In the light of successful lithium alloy anodes, attempts have recently been made to develop alloy anodes for sodium ion storage. Komaba et al.[17] reported a tin polyacrylate anode with a high reversible capacity of 500 $mA\,h\,g^{-1}$, based on the electrochemical alloying/dealloying reactions of sodium–tin intermetallic phase. We developed an Sb/C nanocomposite, which showed nearly full usage of its theoretical capacity of 610 $mA\,h\,g^{-1}$ (storage capacity of 3 Na per formula unit) with an excellent capacity retention of 94% over 100 cycles.[18] This study revealed a feasible strategy for creating high capacity sodium ion storage anodes using elements able to form alloys with sodium.

Elemental phosphorus (P) is a particularly attractive anode material, which can react with three Li or Na atoms to form Li_3P[19–22] and Na_3P[23] compounds, giving a theoretical specific capacity of 2596 $mA\,h\,g^{-1}$. This capacity is probably the highest value that can be expected from all known materials, several times higher than those of Na alloys such as $Na_{15}Sn_4$ (847 $mA\,h\,g^{-1}$),[24,25] $Na_{15}Pb_4$ (485 $mA\,h\,g^{-1}$), Na_3Sb (660 $mA\,h\,g^{-1}$),[18,26] and even twice higher than the electrochemical capacity of metallic sodium (1166 $mA\,h\,g^{-1}$). Recently, Park and Sohn[20] and He and co-workers[21] reported lithium storage behaviors of phosphorus, with a reversible capacity of 600 $mA\,h\,g^{-1}$ and 1000 $mA\,h\,g^{-1}$, respectively, under their experimental conditions. We found that the lithium ion storage capacity of phosphorus depends dramatically on its crystalline structure and morphology, and a reversible three lithium ion storage capacity per phosphorus atom (approximately 2355 $mA\,h\,g^{-1}$) can be realized if the phosphorus forms a composite with conductive carbon to make amorphous nanoparticles.[27] However, there have been no reports of the electrochemical sodium ion storage behavior of phosphorus until now.

Herein, we report for the first time on the synthesis and characterization of an amorphous phosphorus/carbon (a-P/C) nanocomposite with extraordinarily high capacity, high rate capability, and considerable cyclability as a novel anode material for sodium ion batteries.

The a-P/C nanocomposite was synthesized simply by high-energy ball-milling of commercial red phosphorus powder with amorphous carbon black (Super P) at an optimized P/C ratio of 7:3 for 24 hours. Detailed preparation procedures are described in the Experimental Section and the influences of the synthetic conditions on the structure and performance of the resulting P/C composites are given in the Supporting Information (Figures S1,S2). Figure 1a compares the XRD pattern of the a-P/C composite with those of commercial red phosphorus and black phosphorus. The a-P/C composite exhibits a featureless diffraction pattern, completely different from those of crystalline red phosphorus and black phosphorus, indicating the amorphous nature of the sample. The high resolution TEM image (Figure 1b) also shows a disordered structure without any discernible lattice fringe, and its electron diffraction pattern appears as a diffuse ring. This further demonstrates that the original phosphorus particles were crushed and broken into smaller clusters in the carbon matrix during the long and vigorous high-energy ball milling, which lead to the formation of a-P/C, or in other words, highly disperse phosphorus clusters in a carbon matrix.

Our recent work has revealed a large difference in the lithium ion storage behaviors of the different allotropic phases of phosphorus.[27] To validate if this phenomenon is also true for sodium ion storage, we compared the charge–discharge behaviors of a-P/C, red phosphorus, and black phosphorus in sodium cells using sodium disks as the counter electrode and a 1.0 $mol\,L^{-1}$ $NaPF_6$ solution as the electrolyte. The red phosphorus shows a quite large charge (sodium ion insertion) capacity of 897 $mA\,h\,g^{-1}$ (Figure 2) but gives only a negligible discharge (sodium ion removal) capacity of

[*] Dr. J. Qian, Dr. X. Wu, Dr. Y. Cao, Prof. X. Ai, Prof. H. Yang
College of Chemistry and Molecular Science
Wuhan University, Wuhan 430072 (China)
E-mail: hxyang@whu.edu.cn

[**] This work is financially supported by the National 973 Program of China (2009CB220103) and the National Science Foundation of China (21273167).

Supporting information for this article is available on the WWW under http://dx.doi.org/10.1002/anie.201209689.

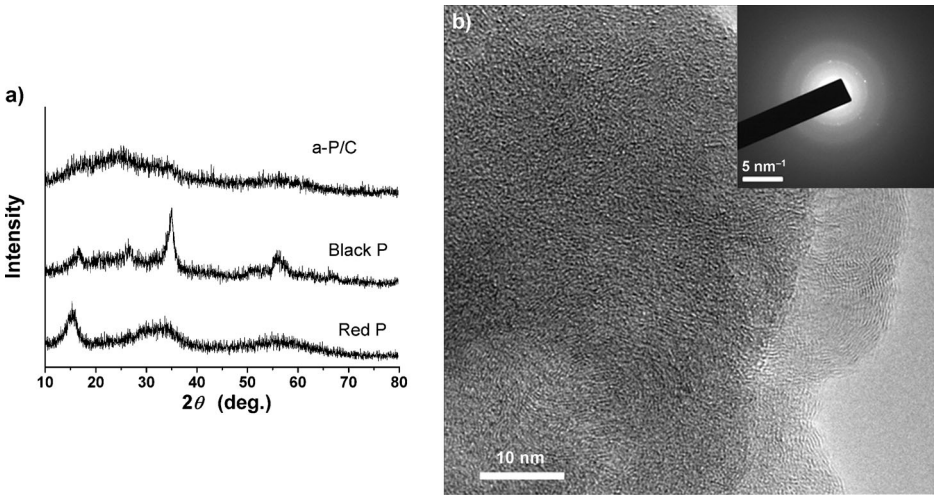

Figure 1. a) XRD pattern of the as-prepared a-P/C composite, compared with that of commercial red phosphorus and black phosphorus, synthesized according to ref. [20]; b) HRTEM image of the a-P/C composite; inset = electron diffraction pattern of a-P/C.

known elements that can store sodium ions. Elemental phosphorus not only has the highest level of theoretical sodium ion storage capacity but also has the highest experimental value of capacity among all the known elements that can store sodium ions. The surprisingly high reversible capacity of the a-P/C composite is several times higher than those reported for carbon or alloy anodes.

Based on these results, we focused our attention on the anodic behavior of the a-P/C composite. Figure 3a shows the cyclic voltammograms (CVs) of the a-P/C composite. During the first cathodic scan, a weak irreversible band appeared at 1.2–0.5 V, corresponding to the electrochemical decomposition of electrolyte for the formation of a solid-electrolyte interface (SEI) film on the electrode surface. When the potential scanned from 0.5 V to 0 V, a large and broad anodic peak emerged as an indication of the sodium ion insertion reaction to form the compounds, Na_xP. In the reversed scan, a number of anodic peaks appeared at 0.53 V, 0.60 V, 0.75 V, and 1.4 V, possibly corresponding to a stepwise sodium ion de-intercalation from the fully charged Na_3P phase to form the Na_2P, NaP, and NaP_7 intermediates, based on the Na/P phase diagram.[23] All the CV peak potentials matched well with the voltage plateaus in the charge/discharge curves in Figure 2 and stayed almost unchanged in subsequent cycles, indicating quite reversible sodium–phosphorus insertion/extraction reactions. Nevertheless, it should be mentioned that the cathodic peaks in the CV curves were not as well separated as their anodic counterparts. This implies a much slower rate of sodium ion insertion than the extraction process, as will be discussed in a later section. Figure 3b gives the voltage profiles of the a-P/C sample for the first five cycles at a constant current of 250 mA h g^{-1}. The charge/discharge curves show three-step

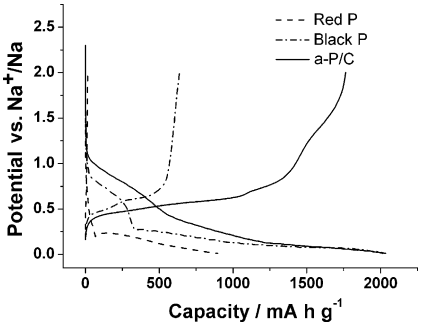

Figure 2. Initial charge/discharge curves of three phases of phosphorus: red phosphorus, black phosphorus, and a-P/C nanocomposite. All the electrodes were tested at a constant current density of 250 mA g^{-1} in the voltage range of 0.01 V–2 V versus Na^+/Na.

Table 1: A comparison of the theoretical and experimental capacities of elements capable of storing sodium ions.

Element	Max. Na content in Na_xX	Vol. ratio of Na_xX/X	T_{cap} [mA h g^{-1}]	$E_{cap.}$ [mA h g^{-1}]
Na	–	–	1166	–
C	$< NaC_6$	< 2%	< 372	200–300[30–31]
Si	NaSi	130%	954	–
Sn	$Na_{3.75}Sn$	525%	847	500[17]
Sb	Na_3Sb	390%	664	610[18]
Pb	$Na_{3.75}Pb$	487%	484	480[17]
P	Na_3P	491%	2596	1764[a]

[a] The current study.

15 mA h g^{-1}, indicating the inactivity of this material for a sodium ion insertion reaction because of its insulating electronic nature. Black phosphorus is known to have higher bulk conductivity[28] and therefore showed a much improved charge capacity of 2035 mA h g^{-1}, which is nearly 80% of its theoretical three sodium ion insertion capacity. However, the reversible discharge capacity of this material is only 637 mA h g^{-1}. This large capacity loss may be ascribed to the enormous volumetric change of 490% from phosphorus to Na_3P, which caused severe pulverization of the material and lead to poor cyclability, as is usually observed in lithium alloy electrodes.[29] In contrast, the a-P/C composite exhibited greatly enhanced electrochemical performance with initial charge/discharge capacities of 2015 mA h g^{-1} and 1764 mA h g^{-1}, respectively, and a very high initial coulombic efficiency of 87%, suggesting that the amorphous structure of the phosphorus can effectively buffer the strong volumetric expansion seen during charge–discharge cycling.

Table 1 compares the theoretical capacities (T_{cap}) and experimentally observed reversible capacities (E_{cap}) for all the

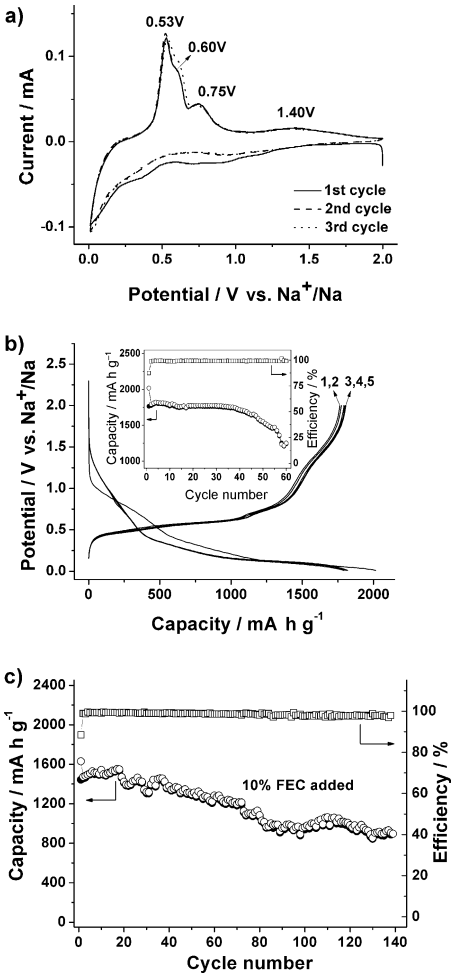

Figure 3. a) CV curves of the a-P/C composites scanned at a rate of 0.02 mV s^{-1}; b) charge–discharge profiles at a constant rate of 250 mA g^{-1}; inset = the change in the reversible capacities with cycle number; c) long-term cycle performance in 1 mol L^{-1} $NaPF_6$ + EC-DEC electrolyte with 10% FEC.

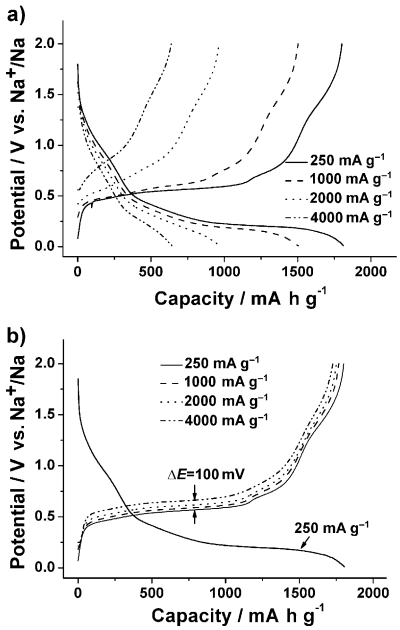

Figure 4. a) Rate performance of the a-P/C sample charged and discharged at the same current density from 250 mA g^{-1} to 4000 mA g^{-1}; b) Voltage profiles of the a-P/C sample charged at a current density of 250 mA g^{-1} and then discharged at a different current density from 250 mA g^{-1} to 4000 mA g^{-1}.

voltage plateaus, which agree very well with the CV peaks in Figure 3a. The reversible capacity of the material reached 1764 mA h g^{-1} during the first cycle and increased to 1800 mA h g^{-1} for the third cycle, simultaneously the coulombic efficiency increased from 87% to 99%. After subsequent cycles, the reversible capacity remained stable at approximately 1750 mA h g^{-1} during the first 40 cycles and then decreased gradually to 1200 mA h g^{-1} at the 60th cycle (see the inset in Figure 3b), possibly because of the volumetric change of the material during repeated sodium ion insertion and extraction, which leads to a breakdown of the SEI film and a loss of electrical contact between the electroactive particles and current collectors. To solve this problem, we added 10% fluoroethylene carbonate (FEC, a strong SEI film-forming additive) in the electrolyte to enhance the structural stability of the SEI film on the anode. As shown in Figure 3c, the reversible capacity remained at 1500 mA h g^{-1} after the first 20 cycles in the FEC-containing electrolyte and then decreased gradually to approximately 1000 mA h g^{-1} at the 80th cycle. Afterwards, the capacity stayed steady for up to 140 cycles. Despite this decay of the capacity, this P/C composite still demonstrated considerable cyclability. We believe that the cycling stability could be greatly enhanced by appropriate structural design of the electrode, optimization of the electrolyte composition, and buffering strategies, as is frequently used for lithium alloy anodes.

Figure 4a shows the rate capability of the a-P/C sample at various charge/discharge currents. At a moderate current of 250 mA g^{-1}, the electrode can deliver a discharge capacity of 1800 mA h g^{-1}, but this capacity decreased considerably to 1380 mA h g^{-1} and 930 mA h g^{-1} when the current rate increased to a high value of 1000 mA g^{-1} and 2000 mA g^{-1}, respectively. At a very high rate of 4000 mA g^{-1}, the discharge capacity was only 640 mA h g^{-1}, showing rapid capacity degradation with increasing current rate. However, careful inspection of the voltage curves revealed that the capacity loss occurred mainly in the low potential plateau of 0.2 V, that is, the charge capacity at the 0.2 V plateau decreased rapidly with increasing current density, which lead to an insufficient charge at high rates. This phenomenon suggests that the sodium ion insertion reaction is slower than the sodium ion extraction reaction, resulting in a large cathodic polarization at increased current rates. The kinetic frustration of the a-P/C material most likely resulted from the poor electronic and ionic conductivities of its reaction intermediates, Na_xP. Electrochemical impedance spectra (Supporting Information, Figure S3) revealed that the charge transfer resistance (R_{ct}) of the sodium ion insertion reaction (approximately 300 Ω) is ten times larger than that of the extraction process (approximately 20 Ω), suggesting that the a-P/C composite is easily

discharged if it is well charged. To confirm this idea, the a-P/C electrode was first charged at a moderate rate of 250 mA g^{-1} and then discharged at various rates from 250 mA g^{-1} to 4000 mA g^{-1}. The discharge capacity varies slightly from 1765 mA h g^{-1} to 1730 mA h g^{-1}, with 98% capacity retention when the discharge rate increases from 1000 mA g^{-1} to 2000 mA g^{-1} (Figure 4b). Even at a very high current of 4000 mA g^{-1}, the a-P/C composite can still maintain a very high capacity of 1715 mA h g^{-1}, 95% of its potential capacity.

In summary, we prepared an amorphorus P/C nanocomposite and tested its feasibility as an anode material for sodium ion batteries. The a-P/C composite displayed a surprisingly high sodium ion storage capacity of 1764 mA h g^{-1}, and considerable cyclability over 100 cycles. To the best of our knowledge, this is the first time such a high capacity and rate capability has been reported for phosphorus anode materials. Combining with the natural abundance and environmental friendliness of phosphorus, the a-P/C composite offers great promise as a high capacity and high rate anodic material for the next generation of sodium ion batteries.

Experimental Section

Materials synthesis and characterization: The amorphous phosphorus/carbon composite was prepared by direct ball milling of red phosphorus powders (99.3% purity) and Super P carbon (TIMCAL Graphite & Carbon) in an optimized mass ratio of 7:3, according to a previously reported procedure.[27] The starting materials were weighed, mixed, and put into a steel vial with 10 mm milling balls. The weight ratio of milling balls to reagent powders was 20:1. The milling vial was filled with argon gas and set in a shaking miller (QM-3A, Nanjing, China). The rotation speed of the miller was set to 1200 rpm for 24 h. Characterization of the active powder was carried out by powder X-ray diffractometry (XRD; Shimadzu XRD-6000, CuKa source) and transmission electron microscopy (JEM-2010HT and JEM-2010FEF).

Electrochemical measurements: The electrochemical measurement of the amorphous phosphorus/carbon as anode-active materials was done using 2032-type coin cells. The working electrode was prepared by coating a slurry containing 80 wt% active material, 10 wt% CMC binder, and 10 wt% Super P on a copper foil substrate. Then the electrode film was dried in an oven at 60 °C overnight. The mass loading of the active material within the film was about 3 mg cm^{-2}. A sodium disk (∅16 mm × 6 mm, approximately 100 mg) served as the counter and reference electrode. The electrolyte used in this work was 1.0 mol L^{-1} $NaPF_6$ in an ethylene carbonate (EC)-diethyl carbonate (DEC) solution, with or without the addition of fluoroethylene carbonate (FEC). All the cells were assembled in a glove box filled with argon and tested at room temperature. The galvanostatic charge/discharge test was conducted on a LAND cycler (Wuhan Kingnuo Electronic Co., China). Cyclic voltammetric measurements were carried out with a coin cell at a scan rate of 0.02 mV s^{-1} using a CHI 660a electrochemical workstation (ChenHua Instruments Co., China). Electrochemical impedance spectra were recorded by an impedance measuring unit (IM 6e, Zahner) with an oscillation amplitude of 5 mV at the frequency range of 100 m Hz to 100 kHz.

Received: December 4, 2012
Revised: December 25, 2012
Published online: March 19, 2013

Keywords: anode material · cyclic voltammetry · rate capability · phosphorus · sodium ion batteries

[1] V. Palomares, P. Serras, I. Villaluenga, K. B. Hueso, J. Carretero-Gonzalez, T. Rojo, *Energy Environ. Sci.* **2012**, *5*, 5884 – 5901.
[2] S.-W. Kim, D.-H. Seo, X. Ma, G. Ceder, K. Kang, *Adv. Energy Mater.* **2012**, *2*, 710 – 721.
[3] N. Yabuuchi, M. Kajiyama, J. Iwatate, H. Nishikawa, S. Hitomi, R. Okuyama, R. Usui, Y. Yamada, S. Komaba, *Nat. Mater.* **2012**, *11*, 512 – 517.
[4] Y. Cao, L. Xiao, W. Wang, D. Choi, Z. Nie, J. Yu, L. V. Saraf, Z. Yang, J. Liu, *Adv. Mater.* **2011**, *23*, 3155 – 3160.
[5] R. Berthelot, D. Carlier, C. Delmas, *Nat. Mater.* **2011**, *10*, 74 – 80.
[6] D. Kim, E. Lee, M. Slater, W. Lu, S. Rood, C. S. Johnson, *Electrochem. Commun.* **2012**, *18*, 66 – 69.
[7] H. Kim, I. Park, D.-H. Seo, S. Lee, S.-W. Kim, W. J. Kwon, Y.-U. Park, C. S. Kim, S. Jeon, K. Kang, *J. Am. Chem. Soc.* **2012**, *134*, 10369 – 10372.
[8] P. Barpanda, T. Ye, S.-i. Nishimura, S.-C. Chung, Y. Yamada, M. Okubo, H. Zhou, A. Yamada, *Electrochem. Commun.* **2012**, *24*, 116 – 119.
[9] B. L. Ellis, W. R. M. Makahnouk, Y. Makimura, K. Toghill, L. F. Nazar, *Nat. Mater.* **2007**, *6*, 749 – 753.
[10] J. Qian, M. Zhou, Y. Cao, X. Ai, H. Yang, *Adv. Energy Mater.* **2012**, *2*, 410 – 414.
[11] J. Qian, M. Zhou, Y. Cao, H. Yang, *J. Electrochem. (Chin. Ed.)* **2012**, *18*, 108 – 112.
[12] Y. H. Lu, L. Wang, J. G. Cheng, J. B. Goodenough, *Chem. Commun.* **2012**, *48*, 6544 – 6546.
[13] M. Zhou, L. M. Zhu, Y. L. Cao, R. R. Zhao, J. F. Qian, X. P. Ai, H. X. Yang, *RSC Adv.* **2012**, *2*, 5495 – 5498.
[14] R. R. Zhao, L. M. Zhu, Y. L. Cao, X. P. Ai, H. X. Yang, *Electrochem. Commun.* **2012**, *21*, 36 – 38.
[15] S. Komaba, W. Murata, T. Ishikawa, N. Yabuuchi, T. Ozeki, T. Nakayama, A. Ogata, K. Gotoh, K. Fujiwara, *Adv. Funct. Mater.* **2011**, *21*, 3859 – 3867.
[16] K. Tang, L. Fu, R. J. White, L. Yu, M.-M. Titirici, M. Antonietti, J. Maier, *Adv. Energy Mater.* **2012**, *2*, 873 – 877.
[17] S. Komaba, Y. Matsuura, T. Ishikawa, N. Yabuuchi, W. Murata, S. Kuze, *Electrochem. Commun.* **2012**, *21*, 65 – 68.
[18] J. F. Qian, Y. Chen, L. Wu, Y. L. Cao, X. P. Ai, H. X. Yang, *Chem. Commun.* **2012**, *48*, 7070 – 7072.
[19] J. Sangster, A. Pelton, H. Okamoto, *J. Phase Equilib.* **1995**, *16*, 92 – 93.
[20] C. M. Park, H. J. Sohn, *Adv. Mater.* **2007**, *19*, 2465 – 2468.
[21] L. Wang, X. He, J. Li, W. Sun, J. Gao, J. Guo, C. Jiang, *Angew. Chem.* **2012**, *124*, 9168 – 9171; *Angew. Chem. Int. Ed.* **2012**, *51*, 9034 – 9037.
[22] L.-Q. Sun, M.-J. Li, K. Sun, S.-H. Yu, R.-S. Wang, H.-M. Xie, *J. Phys. Chem. C* **2012**, *116*, 14772 – 14779.
[23] J. Sangster, *J. Phase Equilib. Diffus.* **2010**, *31*, 62 – 67.
[24] M. K. Datta, R. Epur, P. Saha, K. Kadakia, S. K. Park, P. N. Kumta, *J. Power Sources* **2013**, *225*, 316 – 322.
[25] J. W. Wang, X. H. Liu, S. X. Mao, J. Y. Huang, *Nano Lett.* **2012**, *12*, 5897 – 5902.
[26] L. F. Xiao, Y. L. Cao, J. Xiao, W. Wang, L. Kovarik, Z. M. Nie, J. Liu, *Chem. Commun.* **2012**, *48*, 3321 – 3323.
[27] J. Qian, D. Qiao, X. Ai, Y. Cao, H. Yang, *Chem. Commun.* **2012**, *48*, 8931 – 8933.
[28] A. Morita, *Appl. Phys. A* **1986**, *39*, 227 – 242.
[29] C.-M. Park, J.-H. Kim, H. Kim, H.-J. Sohn, *Chem. Soc. Rev.* **2010**, *39*, 3115 – 3141.
[30] R. Alcántara, P. Lavela, G. F. Ortiz, J. L. Tirado, *Electrochem. Solid-State Lett.* **2005**, *8*, A222 – A225.
[31] D. A. Stevens, J. R. Dahn, *J. Electrochem. Soc.* **2000**, *147*, 1271 – 1273.

